Journal of Linear
and
Topological Algebra

J
L T A

# An implicit finite difference scheme for analyzing the effect of body acceleration on pulsatile blood flow through a stenosed artery

A. R. Haghighi[a*], N. Aliashrafi[b], N. Asghary[c]

[a]*Department of Mathematics, Faculty of shahid beheshti, Urmia Branch Technical and Vocational University(TVU), Tehran, Iran.*
[a,b]*Department of Mathematics, Urmia University of Technology, Urmia, Iran.*
[c]*Department of Mathematics, Central Tehran Branch, Islamic azad university, Tehran, Iran.*

**Abstract.** With an aim to investigate the effect of externally imposed body acceleration on two-dimensional, pulsatile blood flow through a stenosed artery is under consideration in this article. The blood flow has been assumed to be non-linear, incompressible and fully developed. The artery is assumed to be an elastic cylindrical tube and the geometry of the stenosis considered as time dependent, and a comparison has been made with the rigid ones. The shape of the stenosis in the arterial lumen is chosen to be axially non-symmetric but radially symmetric in order to improve resemblance to the in-vivo situations. The resulting system of non-linear partial differential equations is numerically solved using the Crank-Nicolson scheme by exploiting the suitably prescribed conditions. The blood flow characteristics such as the velocity profile, the volumetric flow rate and the resistance to flow are obtained and effects of the severity of the stenosis, the body acceleration on these flow characteristics are discussed. The present results are compared with literature and found to be in agreement.

## 1. Introduction

Global cardiovascular deaths are projected to increase from 16.7 million in 2002 to 23.3 million in 2030 [15]. Among the various cardiovascular diseases, atherosclerosis is one of

---

*Corresponding author.
E-mail address: ah.haghighi@uut.ac.ir (A. R. Haghighi).

the most common of these diseases, which is a constriction due to the multiple plaques formation and the accumulation of fatty material and cholesterol inside the lumen of medium and large sized blood vessels and causes narrowing of the blood vessels. The effect of such constriction significantly reduces blood transport in the region beyond the narrowing. Depending on the location of the stenosed vessel, atherosclerosis can increase risk of myocardial infarction and stroke. Many researchers have noted that the initiation and development of atherosclerosis are strongly related to the blood flow characteristics, and the study of the hemodynamic factors of blood flow through an artery is essential in the understanding and treatment of cardiovascular disease [8, 9, 11, 12, 27, 30].

Deshpande et al. [4] investigated the steady, laminar, and Newtonian blood flow through an axisymmetric stenosed artery. They assumed the artery as a rigid cylindrical tube with a uniform cross section. Chakravarty and Mandal take blood flow as non-linear and incompressible through stenosed artery and investigated the blood flow characteristics. They noted that assumption of rigid of vessels is not acceptable, so the vessels is assumed to be an elastic and the geometry of the stenosis considered as time-dependent [3]. Marques et al. have investigated the pulsatile blood flow in a human artery that the vessel is assumed as being a straight wall tube, and the blood flow is considered to be incompressible and axisymmetric. Also, the effect of pulsatile flow was taken into account by imposing the velocity profile of the cardiac cycle [14]. Belardinelli and Cavalcanti [20] in separate studies presented a mathematical model for the local study of nonlinear, two-dimensional, and unsteady blood motion in tapered arteries. In these two studies, blood flow is assumed as incompressible Newtonian fluid and the geometry of the stenosis is timevariant. In their investigations, nonlinear terms in the Navier Stokes equations were considered and the radial and axial velocity profiles were calculated in the form of power series with less complexity. They studied the effect of several factors such as nonlinearity, severity of the stenosis and wall motion on blood flow characteristics. Ponalagusmy and Selvi have developed a mathematical model for blood flow through arterial stenosis with the two-fluid model, consisting of a core region of Casson fluid and a peripheral layer of Newtonian fluid. They concluded that the downstream of the stenotic regions is more important for the diagnosis of vessel diseases [19].

The flow of blood under the influence of body acceleration is significantly affected, while driving a vehicle or flying in an aircraft, because the blood flow in vibration environment, and due to which there may occur serious health problems such as loss of vision, headache, increase of pulse rate and hemorrhage in face, neck and brain. Sankar and Lee have studied the pulsatile flow of blood through an arterial stenosis by considering blood as a core region of Casson fluid and a peripheral layer of Newtonian fluid under periodic body acceleration [24]. Also Shit and Roy examined the pulsatile flow of blood through a stenosed artery under the influence of periodic body acceleration and then analyzed the heat transfer phenomena with constant blood viscosity [25].

Haghighi and Asl, solved the two-dimensional and pulsatile model of blood flow through a tapered artery with overlapping stenosis by using the explicit scheme and indicated that affects the blood flow characteristics [7]. With the above mentioned discussion, we have investigated the blood flow under the body acceleration. The stenosed artery change in to a rectangular and smooth artery, Actually, it is necessary to transform a real physical domain in to a rectangular computational domain with using the coordinate transformation. Since, the basis of the finite difference is Taylor expansion and it is just on the straight line. So, we have subdivided the rectangular domainin to a network by drawing straight lines parallel to the coordinate axes. The numerical solution is obtained by using finite difference Crank-Nicolson scheme. The variation of flow variables such as velocity, flow rate and resistive to flow with different parameters are

shown diagrammatically and discussed.

## 2. The geometry of the stenosis

Consider a two-dimensional, laminar, unsteady, fully developed and axially symmetric flow of blood through a stenosed artery. Cylindrical polar coordinate system $(r, \theta, z)$ is used to analyze the flow, where $r$ and $z$ are taken along the radial and axial directions respectively, and $\theta$ is taken along the circumferential directions. The geometry of the time variant stenosis is constructed mathematically as: (see Fig 1) [22, 28, 29].

$$R(z,t) = \begin{cases} 1 - A[l_0^{n-1}(z-d) - (z-d)^n]a_1(t), & d \leqslant z \leqslant d + l_0 \\ a_1(t), & \text{otherwise} \end{cases}$$

where $A = \frac{\delta}{R_0 L_0^n} \frac{n^{n(n-1)}}{(n-1)}$, $R(z,t)$ is the radius of the stenosed artery, $R_0$ is the constant radius of the normal artery outside the stenotic region, $L$ is taken to be the finite length of the arterial segment, $l_0$ is the length of the stenosis, $d$ is the upstream length of the artery and $\tau_m$ is the critical height of the stenosis. $n \geqslant 2$ is the parameter representing the asymmetry of the stenosis, where $n = 2$ represents that the stenosis is symmetric. The time variant parameter $a_1(t)$ is given by $a_1(t) = 1 + k_r cos(wt + \varphi)$ [9, 21], where $k_r$ is representing the amplitude parameter and $\varphi$ is the phase angle.

## 3. Mathematical formulation and analysis

Let $(r^*, \theta^*, z^*)$ be the cylindrical polar coordinates system in which $z$ is taken along the axial direction. The velocity components $u^*$ and $v^*$ are taken along the axial and radial directions. The governing equations for the blood flow may be written in the form:

$$\frac{\partial u^*}{\partial z^*} + \frac{\partial v^*}{\partial r^*} + \frac{v^*}{r^*} = 0, \tag{1}$$

$$\rho(\frac{\partial u^*}{\partial t^*} + v^*\frac{\partial u^*}{\partial r^*} + u^*\frac{\partial u^*}{\partial z^*}) =$$

$$-\frac{\partial p^*}{\partial z^*} + \mu(\frac{\partial^2 u^*}{\partial r^{*2}} + \frac{1}{r^*}\frac{\partial u^*}{\partial r^*} + \frac{\partial^2 u^*}{\partial z^{*2}}) + \rho G^*(t^*), \tag{2}$$

$$\rho(\frac{\partial v^*}{\partial t^*} + v^*\frac{\partial v^*}{\partial r^*} + u^*\frac{\partial v^*}{\partial z^*}) =$$

$$-\frac{\partial p^*}{\partial r^*} + \mu(\frac{\partial^2 v^*}{\partial r^{*2}} + \frac{1}{r^*}\frac{\partial v^*}{\partial r^*} + \frac{\partial^2 v^*}{\partial z^{*2}} - \frac{v^*}{r^{*2}}). \tag{3}$$

where $p$ is the pressure, $\rho$ is the density and $\mu$ is the viscosity of the fluid.

For $t^* > 0$, the flow is assumed to have a periodic body vibration $G^*(t^*)$ and has the expression of the form:

$$G^*(t^*) = a^* cos(w_b t^* + \varphi_g). \tag{4}$$

where $a^*$ is the amplitude of body acceleration, $w_b$ is the frequency of body acceleration, and $\varphi_g$ is the phase difference.

The non-dimensional variables are obtained as follows:

$$u = \frac{u^*}{U}, v = \frac{v^*}{U}, r = \frac{r^*}{R_0}, l_0 = \frac{l_0^*}{R_0}, z = \frac{z^*}{R_0},$$

$$t = \frac{t^* U}{R_0}, d = \frac{d^*}{R_0}, p = \frac{p^*}{\rho U^2}, Re = \frac{\rho U R_0}{\mu}.$$

Using non-dimensional variables in the Eqs.(1)-(3) we get: [10, 16, 26]

$$\frac{\partial u}{\partial z} + \frac{\partial v}{\partial r} + \frac{v}{r} = 0, \tag{5}$$

$$\frac{\partial u}{\partial t} + v\frac{\partial u}{\partial r} + u\frac{\partial u}{\partial z} =$$

$$-\frac{\partial p}{\partial z} + \frac{1}{\alpha^2}(\frac{\partial^2 u}{\partial r^2} + \frac{1}{r}\frac{\partial u}{\partial r} + \frac{\partial^2 u}{\partial z^2}) + \frac{1}{\alpha^2}G(t), \tag{6}$$

$$\frac{\partial v}{\partial t} + v\frac{\partial v}{\partial r} + u\frac{\partial v}{\partial z} =$$

$$-\frac{\partial p}{\partial r} + \frac{1}{\alpha^2}(\frac{\partial^2 v}{\partial r^2} + \frac{1}{r}\frac{\partial v}{\partial r} + \frac{\partial^2 v}{\partial z^2} - \frac{v}{r^2}). \tag{7}$$

The non-dimensional parameters appearing in Eqs.(6)-(7) is defined as Womersley parameter $\alpha^2 = \frac{UR_0}{\nu}$ [26].

Using the non-dimensional quantities $a_0 = \frac{R_0^2 a_0^*}{\nu U}$ and $b = \frac{w_b}{w}$, the body acceleration expression defined in the following form [26]:

$$G(t) = a_0 cos(bt + \varphi_g). \tag{8}$$

The dimensionless pressure gradient $\frac{\partial p}{\partial z}$ appearing in Eqs.(5)-(7) is given by [5, 6]:

$$-\frac{\partial p}{\partial z} = A_0 + A_1 cos\omega t, \quad t > 0 \tag{9}$$

where $A_0$ is the constant amplitude of the pressure gradient, $A_1$ is the amplitude of the pulsatile component giving rise to the systolic and diastolic pressures and $w = 2\pi f_p$, $f_p$ is the pulse frequency.

The boundary conditions are:

$$r = 0 : v(r, z, t) = 0, \frac{\partial u(r, z, t)}{\partial r} = 0, \tag{10}$$

$$r = R(z) : v(r, z, t) = \frac{\partial R}{\partial t}, u(r, z, t) = 0. \tag{11}$$

The initial conditions are as follows [10, 17]:

$$u(r, z, 0) = 2\overline{u}[1 - (\frac{r}{R})^2], v(r, z, 0) = 0. \tag{12}$$

where $\overline{u}$ is the mean axial velocity at any given cross section.

## 4.    Transformation of the governing equations

In order to immobilize the vessel wall in the transformed coordinate $\xi$, we introduce the radial coordinate transformation given by $\xi = \dfrac{r}{R}$ [2, 10, 13, 17, 18, 23]. By using this transformation, the constricted tube is transformed into a straight tube. Using this transformation, Eqs.(5)-(7) and prescribed boundary conditions (10)-(12) taken the following form:

$$\frac{\partial u}{\partial t} = -\frac{\partial p}{\partial z} + \frac{1}{R}\frac{\partial u}{\partial \xi}\left[\xi\left(u\frac{\partial R}{\partial z} + \frac{\partial R}{\partial t}\right) - v\right] - u\frac{\partial u}{\partial z}$$

$$+\frac{1}{\alpha^2}\left[\frac{1}{R^2}\left\{1 + (\xi\frac{\partial R}{\partial z})^2\right\}\frac{\partial^2 u}{\partial \xi^2}\right.$$

$$\left.+\frac{1}{\xi R^2}\left\{1 + 2(\xi\frac{\partial R}{\partial z})^2 - \xi^2 R\frac{\partial^2 R}{\partial z^2}\right\}\frac{\partial u}{\partial \xi} + \frac{\partial^2 u}{\partial z^2}\right] + \frac{1}{\alpha^2}G(t), \tag{13}$$

$$\frac{1}{R}\frac{\partial v}{\partial \xi} + \frac{v}{\xi R} + \frac{\partial u}{\partial z} - \frac{\xi}{R}\frac{\partial R}{\partial z}\frac{\partial u}{\partial \xi} = 0, \tag{14}$$

$$\xi = 0 : v(\xi, z, t) = 0, \frac{\partial u(\xi, z, t)}{\partial \xi} = 0, \tag{15}$$

$$\xi = 1 : v(\xi, z, t) = \frac{\partial R}{\partial t}, u(\xi, z, t) = 0, \tag{16}$$

$$u(\xi, z, 0) = 2\overline{u}(1 - \xi^2), z(\xi, z, 0) = 0. \tag{17}$$

In the following the aim is to derive the radial velocity component by using the continuity equation. Multiplying Eq.(14) by $\xi R$ and integrating with respect to $\xi$ between limits 0 to $\xi$, one obtains:

$$\int_0^\xi \xi \frac{\partial v}{\partial \xi} d\xi + \int_0^\xi v d\xi + \int_0^\xi \xi R \frac{\partial u}{\partial z} d\xi - \int_0^\xi \xi^2 \frac{\partial R}{\partial z} \frac{\partial u}{\partial \xi} d\xi = 0, \tag{18}$$

$$\xi v(\xi, z, t) + R \int_0^\xi \xi \frac{\partial u}{\partial z} d\xi - \frac{\partial R}{\partial z} \xi^2 u + \frac{\partial R}{\partial z} \int_0^\xi 2\xi u d\xi = 0, \tag{19}$$

$$v(\xi, z, t) = -\frac{R}{\xi} \int_0^\xi \xi \frac{\partial u}{\partial z} d\xi + \frac{\partial R}{\partial z} (\xi u - \frac{2}{\xi} \int_0^\xi \xi u d\xi). \tag{20}$$

Using the boundary conditions (16) at $\xi = 1$, Eq. (20) becomes:

$$\frac{1}{R} \frac{\partial R}{\partial t} = -\int_0^1 \xi \frac{\partial u}{\partial z} d\xi - \frac{2}{R} \frac{\partial R}{\partial z} \int_0^1 \xi u d\xi. \tag{21}$$

and has the form:

$$\int_0^1 \xi \frac{\partial u}{\partial z} d\xi = -\int_0^1 \frac{2}{R} \frac{\partial R}{\partial z} \xi u d\xi + \int_0^1 \frac{1}{R} \left( \frac{\partial R}{\partial t} \xi f(\xi) \right) d\xi. \tag{22}$$

Where $f(\xi)$ represents an arbitrary function satisfying $\int_0^1 \xi f(\xi) d\xi = 1$. Let $f(\xi)$ is of the form: $f(\xi) = 4(1 - \xi^2)$. Taking the approximation of treating the equality between the integrals to integrands, Eq.(22) can be written as follows:

$$\frac{\partial u}{\partial z} = -\frac{2}{R} \frac{\partial R}{\partial z} u - \frac{4}{R} (1 - \xi^2) \frac{\partial R}{\partial t}. \tag{23}$$

By substituting (22) into (20), the radial velocity component can be obtained as follows:

$$v(\xi, z, t) = \xi \left[ \frac{\partial R}{\partial z} u + \frac{\partial R}{\partial t} \left( 2 - \xi^2 \right) \right]. \tag{24}$$

## 5. Computational scheme

The Crank-Nicolson scheme are carried out for solving Eq.(13). The central difference formula is used to express the spatial derivatives and the forward difference formula is applied to the time derivative and these are given by:

$$\frac{\partial u}{\partial \xi} = \frac{1}{2} \left[ \frac{(u)_{i,j+1}^k - (u)_{i,j-1}^k}{2\Delta\xi} + \frac{(u)_{i,j+1}^{k+1} - (u)_{i,j-1}^{k+1}}{2\Delta\xi} \right], \tag{25}$$

$$\frac{\partial u}{\partial z} = \frac{(u)_{i+1,j}^k - (u)_{i-1,j}^k}{2\Delta z}, \tag{26}$$

$$\frac{\partial^2 u}{\partial \xi^2} = \frac{1}{2} \left[ \frac{(u)_{i,j+1}^k - 2(u)_{i,j}^k + (u)_{i,j-1}^k}{\Delta\xi^2} + \frac{(u)_{i,j+1}^{k+1} - 2(u)_{i,j}^{k+1} + (u)_{i,j-1}^{k+1}}{\Delta\xi^2} \right], \tag{27}$$

$$\frac{\partial^2 u}{\partial z^2} = \frac{(u)_{i+1,j}^k - 2(u)_{i,j}^k + (u)_{i-1,j}^k}{\Delta z^2}, \tag{28}$$

$$\frac{\partial u}{\partial t} = \frac{(u)_{i,j}^{k+1} - (u)_{i,j}^k}{\Delta t}. \tag{29}$$

We define:

$$\begin{cases} \xi_j = (j-1)\Delta\xi, & (j = 1, 2, ..., N+1) \\ z_i = (i-1)\Delta z, & (i = 1, 2, ..., M+1) \\ t_k = (k-1)\Delta t, & (k = 1, 2, ...) \end{cases}$$

where $\Delta\xi$, $\Delta z$, $\Delta t$ are the increments in the radial, the axial and the time directions respectively. Using the presented transformation and the Crank-Nicolson scheme, Eqs.(13), take the following forms:

$$A_{i,j} u_{i,j-1}^{k+1} + B_{i,j} u_{i,j}^{k+1} + C_{i,j} u_{i,j+1}^{k+1} = D_{i,j}, \tag{30}$$

$$A_{i,j} = \frac{\Delta t}{4R_i^k \Delta \xi}[\xi_j(u_{i,j}(\frac{\partial R}{\partial z})_i^k + (\frac{\partial R}{\partial t})_i^k) - v_{i,j}] - \frac{\Delta t}{2\alpha^2(R_i^k)^2\Delta\xi^2}\{1 + (\xi_j(\frac{\partial R}{\partial z})_i^k)^2\}$$

$$+ \frac{\Delta t}{4\alpha^2(R_i^k)^2\xi_j\Delta\xi}\{1 + 2(\xi_j(\frac{\partial R}{\partial z})_i^k)^2 - \xi_j^2 R_i^k(\frac{\partial^2 R}{\partial z^2})_i^k\},$$

$$B_{i,j} = 1 + \frac{\Delta t}{\alpha^2(R_i^k)^2\Delta\xi^2}\{1 + (\xi_j(\frac{\partial R}{\partial z})_i^k)^2\},$$

$$C_{i,j} = \frac{-\Delta t}{4R_i^k \Delta \xi}[\xi_j(u_{i,j}(\frac{\partial R}{\partial z})_i^k + (\frac{\partial R}{\partial t})_i^k) - v_{i,j}] - \frac{\Delta t}{2\alpha^2(R_i^k)^2\Delta\xi^2}\{1 + (\xi_j(\frac{\partial R}{\partial z})_i^k)^2\}$$

$$- \frac{\Delta t}{2\alpha^2(R_i^k)^2\xi_j\Delta\xi}\{1 + 2(\xi_j(\frac{\partial R}{\partial z})_i^k)^2 - \xi_j^2 R_j^k(\frac{\partial^2 R}{\partial z^2})_i^k\}],$$

$$D_{i,j} = u_{i,j}^k - \Delta t(\frac{\partial R}{\partial z}) + \frac{\Delta t}{4R_i^k \Delta \xi}((u)_{i,j+1}^k - (u)_{i,j-1}^k)[\xi_j(u_{i,j}(\frac{\partial R}{\partial z})_i^k + (\frac{\partial R}{\partial t})_i^k)$$

$$- v_{i,j}] - \frac{\Delta t}{2\Delta z}(u)_{i,j}^k((u)_{i+1,j}^k - (u)_{i-1,j}^k) + \frac{\Delta t}{2\alpha^2(R_i^k)^2\Delta\xi^2}((u)_{i,j+1}^k - 2(u)_{i,j}^k$$

$$+ (u)_{i,j-1}^k)\{1 + (\xi_j(\frac{\partial R}{\partial z})_i^k)^2\} + \frac{\Delta t}{4\alpha^2(R_i^k)^2\xi_j\Delta\xi^2}\{1 + 2(\xi_j(\frac{\partial R}{\partial z})_i^k)^2 - \xi_j^2 R_i^k(\frac{\partial^2 R}{\partial z^2})_i^k\}$$

$$((u)_{i,j+1}^k - (u)_{i,j-1}^k) + \frac{\Delta t}{\alpha^2\Delta z^2}((u)_{i+1,j}^k - 2(u)_{i,j}^k + (u)_{i-1,j}^k) + \Delta t(\frac{G(t)}{\alpha^2}).$$

After computing the velocity distribution in the flow domain, one can compute the volumetric flow rate ($Q$), and the resistive impedance ($\Lambda$) by using the following formulas[1, 6]:

$$Q_i^k = 2\pi(R_i^k)^2 \int_0^1 \xi_j(u)_{i,j}^k d\xi_j, \tag{31}$$

$$\Lambda_i^k = \frac{|L(\frac{\partial p}{\partial z})_i^k|}{Q_i^k}. \tag{32}$$

## 6. Numerical results and discussion

Numerical computations have been carried out using the following parameter values [3, 10, 18]:

$$\Delta t = 0.001, \Delta \xi = 0.0125, \Delta z = 0.1, d = 10, R_0 = 1.52, b = 1,$$
$$L = 30, l_0 = 14, A_0 = 0.1, A_1 = 0.2A_0, \alpha = 4,$$
$$k_r = 0.05, \varphi_g = \frac{\pi}{4}, \varphi = 0, f_p = 1.2.$$

Figure 2 shows the axial velocity profile for the stenosed artery at a specific location of $z = 17$ in the stenotic region. According to Fig 2, the numerical method is compared with the corresponding results obtained by Shaw et al. [23] and Mandal et al. [13] at the time $t = 2$ and $\tau_m = 0.2R_0$. The present results are in agreement with Shaw et al. and Mandal et al.

Figure 3 illustrates the dimensionless axial velocity profiles of the flowing blood for different stenosis sizes at $t = 3$ and $n = 2$. Fig 3 depicted that the axial velocity decreases by increasing the size of stenosis. The present figure also includes the axial velocity at the time $t = 2$ through an elastic and rigid artery that the axial velocity in rigid artery is more than the axial velocity in elastic artery and this shows the importance of the assumption of elastic nature of blood arteries.

Figures 4 give the variation of the axial velocity for different amplitudes of body acceleration at the time $t = 3$ and $\tau_m = 0.2R_0$ and $n = 2$. It is observed from Fig 4 that the axial velocity increases as the amplitude of body acceleration increases. Thus, in the presence of vibration, environmental system may produce an increase in blood velocity.

The rate of flow in the stenosed artery for different the stenosis size. It is seen that the flow rate through the elastic artery at the time $t = 3$, $n = 2$ is less than the flow rate through the rigid artery. Also, the rate of flow decreases with the increase in the stenosis size. It is clear that, the volumetric flow rate behavior is corresponding to the geometry of the stenosis so that, at the onest of the stenosis volumetric flow rate dropped and at the stenosis critical height reaches to its lowest level.

The variation of the flow rate with time, for different amplitudes of body acceleration is illustrated in Fig 6. According to this figure, the flow rate increases with the increase of amplitudes of body acceleration. Thus, the volumetric flow has an enhancing effect with its peak value of oscillation on the vibration environmental system.

Figure 7 displays the flow rate through a stenosed artery for different parameters asymmetry of the stenosis at time $t = 3$. According to this figure, the flow rate increases with the increase in the parameters asymmetry of the stenosis.

The resistive impedance in the stenosed artery for different stenosis sizes at the time $t = 3$ and $n = 2$ is shown in Fig 8. According to this figure, the resistive impedance increases with the increase in the stenosis size. Moreover, comparing the resistive impedance of elastic and rigid arteries indicates that the impedance of the elastic artery is more than the rigid artery.

Resistive impedance with time through a stenosed artery for different amplitudes of body acceleration at the time $t = 3$ is presented in Fig 9. In this figure the resistive impedance decreases with the increase of amplitudes of body acceleration. Considering Eq.(32) the volumetric flow rate and the resistive impedance are inversely related.

Figures 10 shows the profiles for resistive impedance is stenosed artery with three

different parameters asymmetry of the stenosis at time $t = 3$. It is clear that the resistive impedance decreases by increasing the parameters asymmetry of the stenosis.

Fig.11 depicts the blood flow patterns for different values of parameters asymmetry of the stenosis and stenosis size. Panels (a) and (b) show flow pattern for the stenosis artery $\tau_m = 0.2R_0$ and $\tau_m = 0.7R_0$ at the time t=3. Obviously, increasing the size of stenosis at t=3 leads to the decrease of the flow lines, thus, increasing the size of stenosis gives rise to the decrease of the axial velocity. Panel (c) and (d) describes the flow lines for the parameters asymmetry of the stenosis n=4 and n=11 at the time t=3.

## 7.  Conclusions

The two-dimensional, unsteady and laminar blood flow through a stenosed artery has been studied. Using the Crank-Nicolson method, the discretized form of the velocity profile, the volumetric flow rate and the resistive impedance have been achieved. The influences of the effective parameters on flow characteristics such as the velocity profile, the volumetric flow rate and the resistive to flow, under the periodic body acceleration, are examined. The blood flow characteristics through elastic artery has been compared with the rigid ones and this difference between the axial velocity of the rigid and the elastic arteries shows the important of the assumption of elastic blood vessels. The results demonstrate that the axial velocity and the rate of flow decrease with the increase in the stenosis size. For this reason, the rate of flow and the resistive impedance are inversely related with the increase in the amplitudes of body acceleration.

## References

[1] N. Ali, A. Zaman, M. Sajid, Unsteady blood flow through a tapered stenotic artery using Sisko model, Comput Fluids. 101 (2014), 42-49.
[2] E. Belardinelli, S. Cavalcanti, A new nonlinear two-dimensional model of blood motion in tapered and elastic vessels, Computers in Biology and Medicine. 21 (1991), 1-13.
[3] S. Chakravarty, P. K. Mandal, Two-dimensional blood flow through tapered arteries under stenotic conditions, International Journal of Non-Linear Mechanics. 35 (5) (2000), 779-793.
[4] M. Deshpande, D. Giddens, F. Mabon, Steady laminar flow through modelled vascular stenoses, J. Biomech. 9 (1976), 165-174.
[5] A. R. Haghighi, S. A. Chalak, Mathematical modeling of blood flow through a stenosed artery under body acceleration, Journal of the Brazilian Society of Mechanical Sciences and Engineering. 39 (7) (2017), 2487-2494.
[6] A. R. Haghighi, M.S. Asl, Mathematical modeling of micropolar fluid flow through an overlapping arterial stenosis, International Journal of Biomathematics. (8) (4) (2015), —.
[7] A. R. Haghighi, M. S. Asl, and M. Kiyasatfar, Mathematical modeling of unsteady blood flow through elastic tapered artery with overlapping stenosed, Journal of the Braziliam Society of Mechanical Sciences and Engineering. (2014) .
[8] H. A. Hogan, M. Henriksen, An evaluation of a micropolar model for blood flow through an idealized stenosis, J Biomech. 22 (3) (1989) 21-218
[9] M. Ikbal, S. Chakravarty, K. Wong, J. Mazumdar, P. Mandal, Unsteady response of Non-Newtonian blood flow through a stenosed artery in magnetic field, Journal of Computational and Applied Mathematics. 230 (1) (2009), 243-259.
[10] M. Ikbal, S. Chakravarty, P. Mandal, Two-layered micropolar fluid flow through stenosed artery: effect of peripheral layer thickness, Computers andt Mathematics with Applications. 58 (7) (2009), 1328-1339.
[11] Z. Ismail, I. Abdullah, N. Mustapha, A. Amin, A power-law model of blood flow through a tapered overlapping stenosed artery, Appl Math Comput. 195 (2013), 669-680.
[12] G. Liu, X. Wang, B. Ai, L. Liu, numerical study of pulsating flow through a tapered artery with stenosis, Chin J Phys. 42 (2012), 401-409.
[13] P. Mandal, S. Chakravarty, A. Mandal, A. Amin, Effect of body acceleration on unsteady pulsatile flow of non-Newtonian fluid through a stenosed artery, Applied Mathematics and Computation. 189 (2007), 766-779.
[14] P. F. Marques, M. E. C. Oliveira, A. S. Franca, M. Pinotti, Modeling and simulation of pulsatile blood flow with a physiologic wave pattern, Artif Organs. 27 (5) (2003), 458-478.
[15] C. D. Mathers, and D. Loncar, Projections of global mortality and burden of disease from 2002 to 2030, PLoS Med. 3 (11) e442 (2006).

[16] J.C. Misra, and G. C. Shit, Flow of a biomagnetic viscoelastic fluid in a channel with stretching walls, Journal of Applied Mechanics. 76 (6) (2009), 061006.

[17] S. Mukhopadhyay, and G. Layek, Numerical modeling of a stenosed artery using mathematical model of variable shape, AAM Intern. 3(6) (2008) 308-328.

[18] N. Mustapha, N. Amin, S. Chakravarty, P. Mandal, Unsteady magnetohydrodynamic blood flow through irregular multi-stenosed arteries, Computers in Biology and Medicine. 39 (2009), 896-906.

[19] R. Ponalagusamy, R. Tamil Selvi, A study on two-layered model (Casson-Newtonian) for blood flow through an arterial stenosis: axially variable slip velocity at the wall, Journal of the Franklin Institute. 348 (9) (2011), 2308-2321.

[20] J. Prakash, and A. Ogulu, A study of pulsatile blood flow modeled as a power law fluid in a constricted tube, Int Commun Heat Mass. 34 (2007), 762-768.

[21] D. Sankar, U. Lee, FDM analysis for MHD flow of a non-Newtonian fluid for blood flow in stenosed arteries, J. Mech. Sci. Technol. 25 (10) (2001), 2573-2581.

[22] D. Sankar, U. Lee, Mathematical modeling of pulsatile flow of non-Newtonian fluid in stenosed arteries, Communications in Nonlinear Science and Numerical Simulation. 14 (7) (2009), 2971-2981.

[23] S. Shaw, P. Murthy, S. Pradhan, P. Mandal, The effect of body acceleration on two dimensional flow of Casson fluid through an artery with asymmetric stenosis, The Open Transport Phenomena Journal. 2 (2010), 55-68.

[24] D.S. Shankar, U. Lee, Nonlinear mathematical analysis for blood flow in a constricted artery under periodic body acceleration, Communications in Nonlinear Science and Numerical Simulation. 16 (11) (2011), 4390-4402.

[25] G. C. Shit, M. Roy, Pulsatile flow and heat transfer of a magneto-micropolar fluid through a stenosed artery under the influence of body acceleration, Journal of Mechanics in Medicine and Biology. 11 (03) (2011), 643-661.

[26] G. C. Shit, S. Majee, Pulsatile flow of blood and heat transfer with variable viscosity under magnetic and vibration environment, Journal of Magnetism and Magnetic Material. 388 (2015), 106-115.

[27] S. Siddiqui, N. Verma, S. Mishra, R. Gupta, Mathematical modelling of pulsatile flow of Cassons fluid in arterial stenosis, Appl Math Comput. 210 (1) (2009), 1-10.

[28] S. Singh, Numerical modeling of two-layered micropolar fluid through an normal and stenosed artery, IJE-Transactions A: Basics. 24 (2) (2011), 177.

[29] N. Srivastava, The Casson fluid model for blood flow through an inclined tapered artery of an accelerated body in the presence of magnetic field, Int. J. Biomedical Engineering and Technology. 15 (3) (2014), 70-91.

[30] G. Zendehbudi, M. Moayeri, Comparison of physiological and simple pulsatile flows through stenosed arteries, J Biomech. 32 (1999), 959-965.
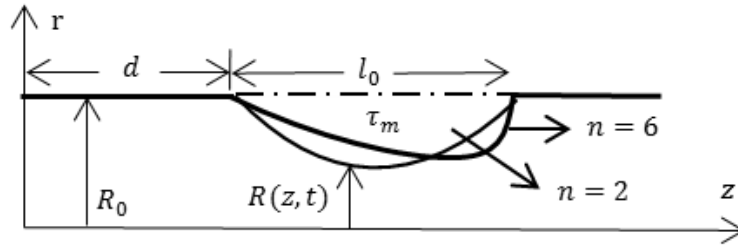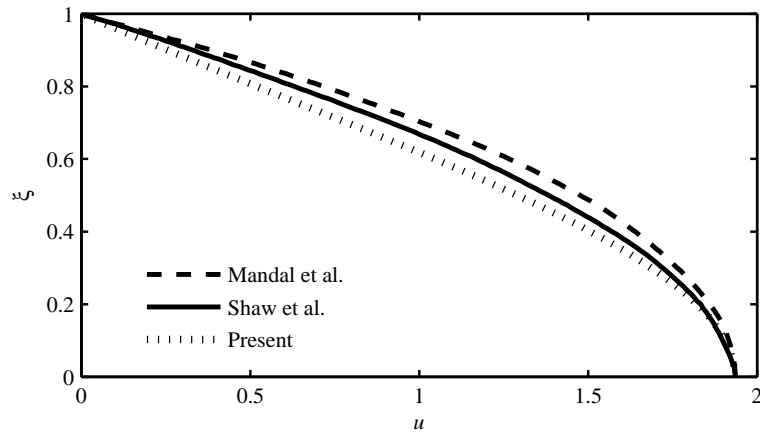
Figure 1. Geometry of the stenosed artery



Figure 2. Comparison of the dimensionless axial velocity profile (z=17, t=2, $\tau_m = 0.2R_0$, n=2)
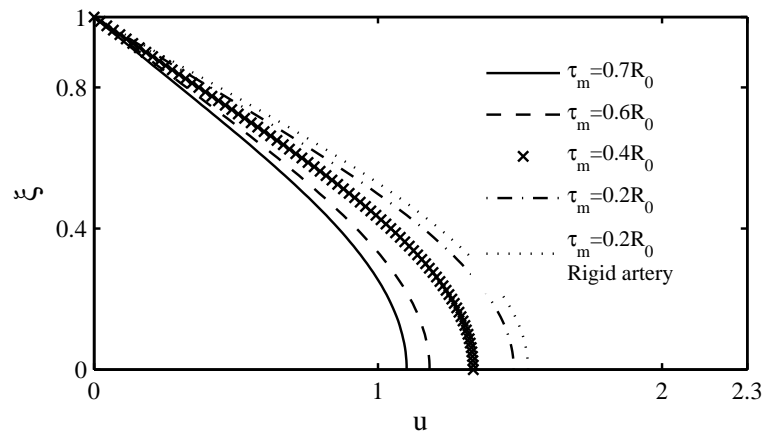


Figure 3. Dimensionless axial velocity profile for different stenosis size (t=3, n=2, $a_0 = 1$)
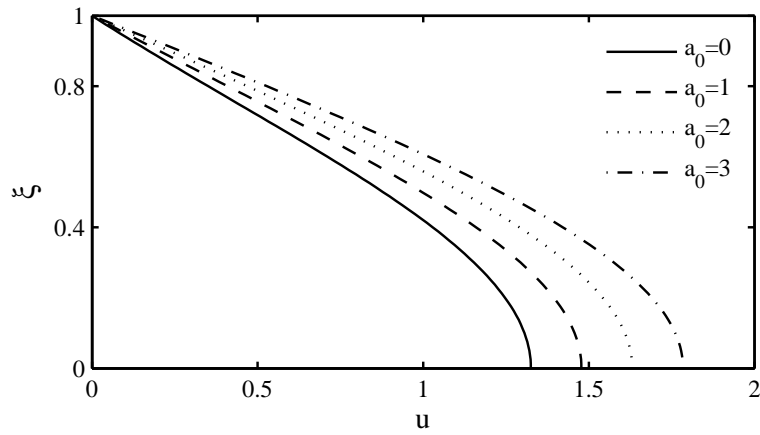
Figure 4. Dimensionless axial velocity profile for different amplitudes of body acceleration (t=3, $\tau_m = 0.2R_0$, n=2)
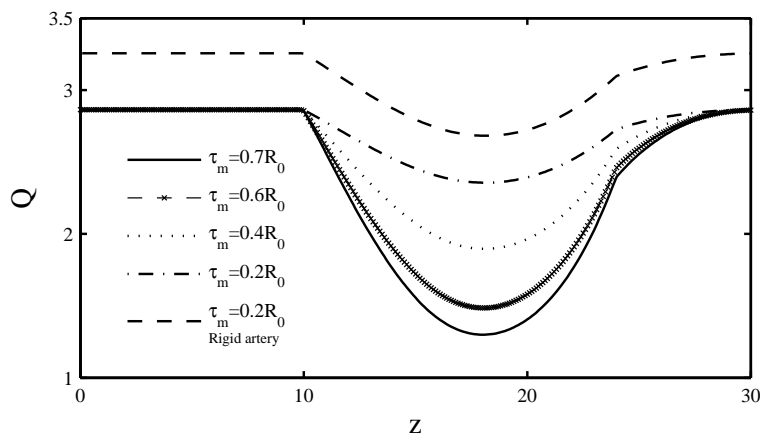


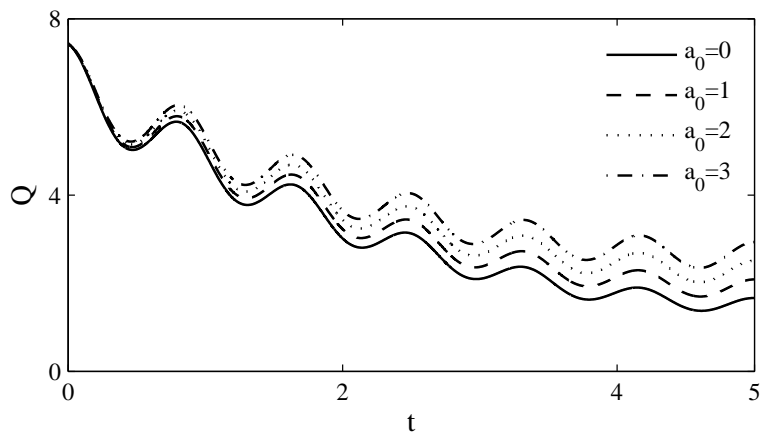Figure 5. Distribution of the rate of flow for different stenosis size (t=3, n=2, $a_0 = 1$)



Figure 6. Distribution of volumetric flow rate with time for different amplitudes of body acceleration ($\tau_m = 0.2R_0$, n=2)
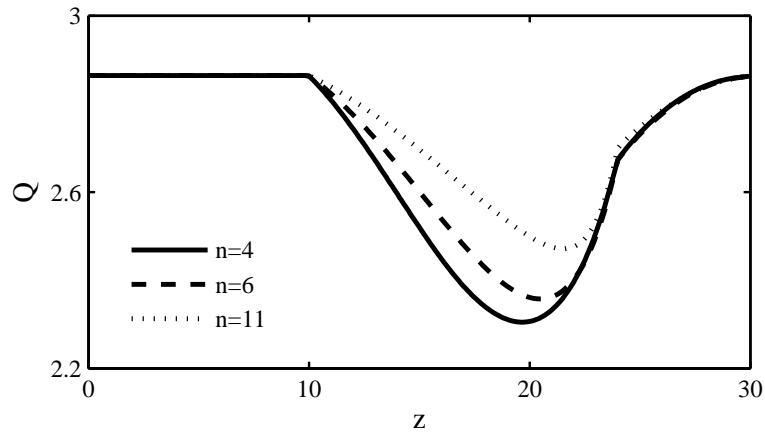
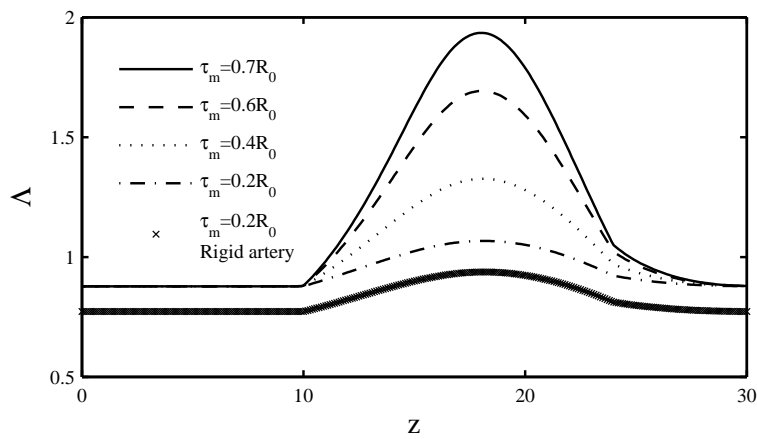Figure 7.   The volumetric flow rate for different parameters asymmetry of the stenosis (t=3, $\tau_m = 0.2R_0$, $a_0 = 1$)



Figure 8. Distribution of the resistive impedance for different stenosis size (t=3, n=2, $a_0 = 1$)
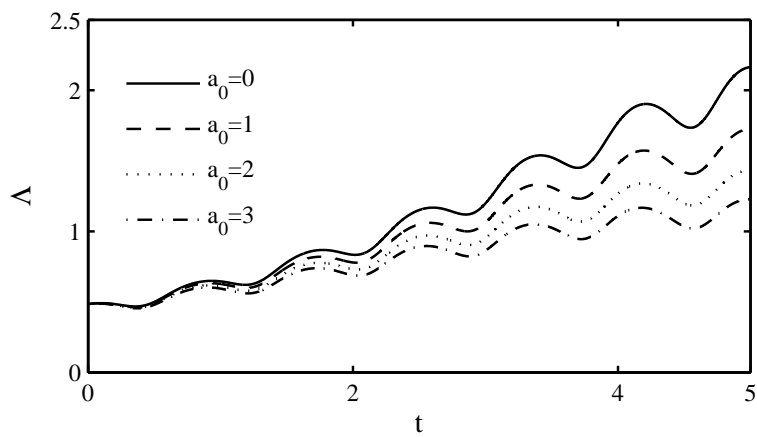


Figure 9.   Distribution of the resistive impedance with time for different amplitudes of body acceleration ($\tau_m = 0.2R_0$, n=2)
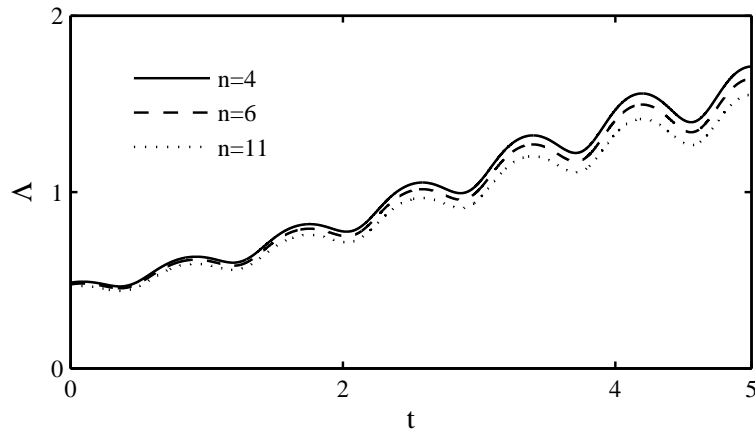
Figure 10.   Distribution of the resistive impedance for different parameters asymmetry of the stenosis ($\tau_m = 0.2R_0$, $a_0 = 1$)
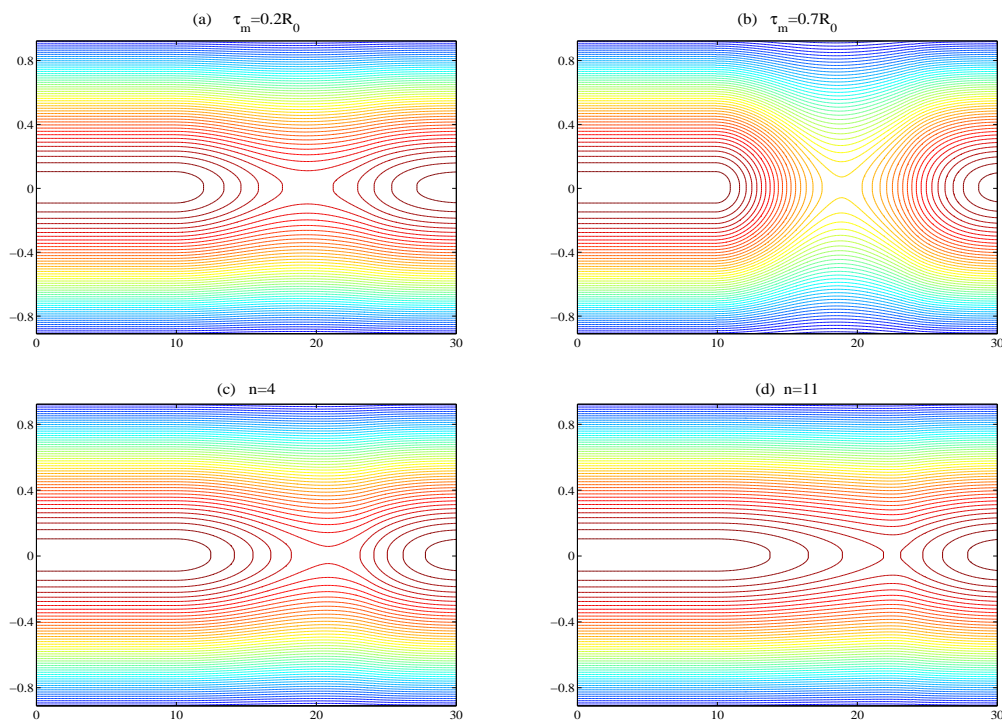


Figure 11. Instantaneous flow patterns of streaming blood (t=3, n=2, $a_0 = 1$)